



Temperature controlled Lévy flights of minority carriers in photoexcited bulk n -InP



Arsen V. Subashiev*, Oleg Semyonov, Zhichao Chen, Serge Luryi

Department of Electrical and Computer Engineering, State University of New York at Stony Brook, Stony Brook, NY 11794-2350, USA

ARTICLE INFO

Article history:

Received 1 November 2013

Accepted 9 November 2013

Available online 13 November 2013

Communicated by V.M. Agranovich

Keywords:

Anomalous diffusion

Lévy flight statistics

Photoluminescence

ABSTRACT

We study by photoluminescence the spatial distribution of minority carriers (holes) arising from their anomalous photon-assisted diffusion upon photo-excitation at an edge of n -InP slab for temperatures ranging from 300 K to 78 K. Giant enhancement in the spread of holes – over distances exceeding 1 cm from the excitation edge – is seen at lower temperatures. We show that the experiment provides a realization of the “Lévy flight” random walk of holes, in which the Lévy distribution index γ is controlled by the temperature. The variation $\gamma(T)$ is close to that predicted earlier, $\gamma = 1 - \Delta/kT$, where $\Delta(T)$ is the Urbach tailing parameter of the absorption spectra. This theoretical prediction is based on the assumption of a quasi-equilibrium intrinsic emission spectrum in the form due to van Roosbroeck and Shockley.

© 2013 Elsevier B.V. All rights reserved.

1. Introduction

Among various stochastic processes, random walk of the Lévy-flight type has gained importance in diverse fields, including hydrodynamics [1], biology [2], financial markets [3], earth sciences [4], etc. It has also found applications to transport of photons, mediated by multiple absorption–reemission processes, in atomic vapors [5] and in astrophysics [6]. In all formerly studied cases, the microscopic ingredient of the anomalous diffusive behavior, the single step distribution (SSD), was hard to access experimentally (with the only exception of hot vapors [5]). Experimental control of the SSD is at best prohibitively difficult, cf. the ingenious artificial media constructed for optical observation of Lévy flight [7].

Lack of control and the experimental uncertainty in the SSD impedes unambiguous interpretation of the data collected with a limited dynamic range, so that the obtained parameters become questionable [8] and even the conclusions subject to overturning [9]. Due to its non-local nature, the Lévy-flight dynamics depends in a nontrivial manner on the boundary conditions [10], on the SSD truncation [11], as well as on the dimensionality of the system [12]. These effects, critically sensitive to the SSD, have been actively studied but mostly theoretically until now. An easily reproducible model system with controlled SSD would render these subtle effects available for experimental studies.

Here we present a simple experimental system exhibiting Lévy flight with the power-law distribution index controlled in a wide range by the ambient temperature. The system itself was recently

discovered [13] in studying photon-assisted transport of minority carriers in semiconductors (photo-excited holes in n -type InP).

In the normal transport process, the stationary distribution of minority carriers produced by optical excitation in semiconductors decays exponentially from the excitation area and is characterized by a micron-scale diffusion length l . However, in moderately-doped direct-gap semiconductors with high radiative efficiency, the minority-carrier transport is strongly modified by the “photon recycling” process (repeated radiative recombination and reabsorption of emerging photons). The distribution of steps in this photon-mediated random walk of minority carriers is defined by the photon reabsorption probability [13] and the single-step probability distribution $\mathcal{P}(x)$ can be calculated from the interband absorption and radiative recombination spectra, which gives [14,15]

$$\mathcal{P}(x) = \frac{\gamma x_{\min}^{\gamma}}{(x_{\min} + |x|)^{1+\gamma}}, \quad (1)$$

where γ is referred to as the distribution index and x_{\min} ($\approx 0.1 \mu\text{m}$) is a parameter determined by the absorption coefficient at high energies, far from the band edge. The SSD (1) asymptotically obeys the power law [14] $\mathcal{P}(x) \sim 1/x^{1+\gamma}$ that results from the anomalously large reabsorption length at the red edge of the spectra in the Urbach-tail region.

The distribution (1) turns out to be “heavy-tailed,” $\gamma \leq 1$ [13–15]. Therefore, the diffusivity [conventionally defined through the second moment of $\mathcal{P}(x)$] diverges and the random walk is governed by rare but large steps. This kind of transport is known as the Lévy flight [16–18].

The resultant power-law stationary spatial distribution is “truncated” by the loss of photons in the free-carrier absorption (FCA) and further modified by the loss of minority carriers in

* Corresponding author.

E-mail address: arsen.subashiev@stonybrook.edu (A.V. Subashiev).

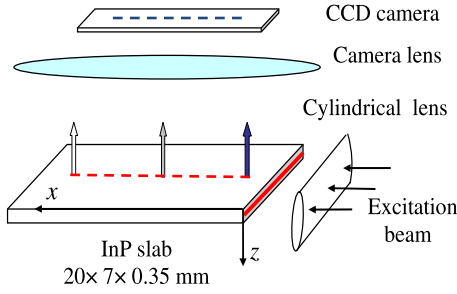


Fig. 1. (Color online.) Edge excitation geometry: laser beam is focused on a narrow strip on the edge side of the sample, while the luminescence is captured from the broadside to project the image on a CCD camera.

non-radiative recombination. In n -doped InP the room-temperature FCA coefficient is $\alpha_{\text{FCA}} [\text{cm}^{-1}] \approx 1.3 \times 10^{-18} N_{\text{D}} [\text{cm}^{-3}]$ and decreases further at lower temperatures [19,20]. Thus, for moderately doped samples this mechanism of loss is ineffective. The relative rates of recombination are characterized by the radiative efficiency $\eta = \tau_{\text{nr}} / (\tau_{\text{nr}} + \tau_{\text{rad}})$ (where τ_{rad}^{-1} and τ_{nr}^{-1} are, respectively, the radiative and non-radiative recombination rates). The average number of steps is given by the recycling factor $\Phi = \eta / (1 - \eta)$, which is typically $\Phi \gg 1$.

In the earlier study [13], we directly observed the power-law decay of the hole concentration, characteristic of a Lévy flight, as a function of the distance from the excitation – up to several millimeters – for differently doped samples at 300 K. Here we demonstrate that the index γ of the Lévy distribution can be controlled by varying the temperature. The decrease of γ at lower T produces further enhancement in the hole spread, reaching centimeter-scale distances.

2. Experiment

The temperature-dependent luminescence was studied in the edge excitation geometry illustrated in Fig. 1 (see also [13]), using n -InP slab [21] of size 20 mm by 7 mm and thickness $d = 350 \mu\text{m}$, corresponding to x , y , and z directions, respectively. The moderate doping level $N_{\text{D}} = 3 \times 10^{17} \text{ cm}^{-3}$ gives optimum radiative efficiency at room temperature [15]. A 808 nm laser beam was focused on the 7 mm edge by a cylindrical lens producing a uniform excitation along the edge. The excitation energy $E = 1.53 \text{ eV}$ was well above InP bandgap ($E_{\text{g}} \approx 1.35 \text{ eV}$) and generated holes only in a submicron layer near the edge. We registered the intensity and spectra of luminescence emitted from the broadside as a function of the distance x from the photo-excited edge.

The edge-excited photoluminescence spectrum for $T = 296 \text{ K}$, recorded at $x = 1 \text{ mm}$, is shown in Fig. 2. Also shown is the luminescence spectrum, observed from the broadside in reflection geometry [15,14]. We note that, compared to the reflection spectrum, the edge-excitation spectrum is noticeably shifted to the red side, indicating substantial filtering [13].

It is important to note that the luminescence spectra retain identical shape in the whole range x . This observation remains valid for all temperatures studied.

The absorption spectrum $\alpha(E)$ of the sample is shown in Fig. 2 by the dash-dotted line. In the whole range of temperatures studied, the red wing of $\alpha(E)$ exhibits an exponential Urbach behavior [19],

$$\alpha_i(E) = \alpha_0 \exp\left[\frac{E - E_{\text{g}}}{\Delta(T)}\right], \quad E < E_{\text{g}} \quad (2)$$

extending down to $\alpha(E) \approx \alpha_{\text{FCA}}$. At $E \geq E_{\text{g}}$, the Urbach exponent saturates. Note that – in contrast to the intrinsic emission spec-

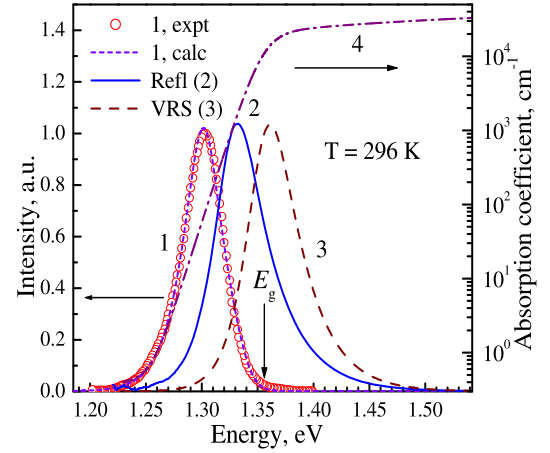


Fig. 2. (Color online.) Luminescence spectra of n -doped InP sample. Photoluminescence spectra (1) for edge excitation and front-side observation; experimental data (circles) are practically indistinguishable from the calculation (dashed line) that allows for spectral filtering. Reflection luminescence spectra from the front side is shown by the solid line (2). The van Roosbroek–Shockley intrinsic emission spectrum, Eq. (3) is shown by the dashed line (3). The dash-dotted line (4) corresponds to the absorption coefficient.

trum – the luminescence spectra observed with the edge excitation are fully in the Urbach tail region of $\alpha(E)$.

Assuming a quasi-equilibrium energy distribution of holes, the intrinsic emission spectrum is given by the well-known van Roosbroek–Shockley (VRS) relation [22],

$$S_{\text{VRS}}(E) \sim \alpha_i(E) E^3 \exp\left(-\frac{E}{kT}\right). \quad (3)$$

The VRS spectrum is also shown in Fig. 2. It has a maximum above E_{g} . Owing to the rapid energy relaxation of holes, the intrinsic emission spectrum in n -InP is well described by Eq. (3), both at room and lower temperatures, with a noticeable deviation in shape only at $T \leq 78 \text{ K}$. The observed red-shifted spectrum $S(E)$ is shaped by reabsorption of luminescence on its way out of the sample, $S(E) = S_{\text{VRS}} \times F(E)$, where $F(E)$ is the spectral filtering function $F(E) = F_1(E)T(E)$ that depends on the hole distribution $p(z)$ across the wafer and is affected by reflections from the sample surfaces. The one-pass filtering function $F_1(E)$ is given by [14, 15]

$$F_1(E) = \int_0^d p(z) \exp[-\alpha(E)z] dz. \quad (4)$$

The factor $T(E) = [1 - R \exp(-\alpha(E)d)]^{-1}$ accounts for the multiple surface reflections; $R \approx 0.33$. Note that due to the high index contrast the radiation escape cone is narrow, i.e. the outgoing radiation propagates close to the normal direction to the surface. Effects of multiple reflections are noticeable only in the far red wing of the spectrum. For the edge excitation, the hole distribution across the sample is nearly homogeneous. Therefore, the typical radiation escape distance in this geometry is much larger and produces considerably larger red shift of the spectrum than for the reflection geometry, where holes are generated near the surface. The filtered spectra, calculated using the VRS relation, are shown in Fig. 2 by the dashed line (1), demonstrating excellent agreement with the experiment [23,24].

The luminescence intensity distributions $I(x)$ were obtained by scanning the CCD image along a line parallel to x (some details can be found in [13]). The proportionality $p(x) \propto I(x)$ is supported by the good agreement between the calculated and observed luminescence spectra for edge excitation.

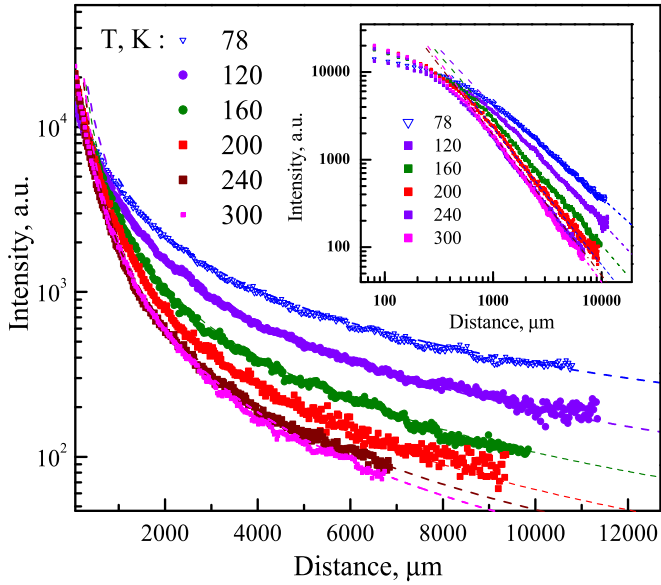


Fig. 3. (Color online.) Distribution of the luminescence intensity $I(x)$ and the hole concentration $p(x) \propto I(x)$ for different temperatures T . Dashed lines correspond to the power-law (1) fitting with an index γ . The inset shows the same distributions in log–log scale.

The resulting distributions for temperatures ranging from 300 K to 78 K are shown in Fig. 3. One can see a huge enhancement of the hole spread that extends over 1 cm at temperatures below 200 K.

The power law $p(x) \sim 1/x^{1+\gamma}$ is clearly observed for all temperatures at distances $x > 0.5$ mm. This is best seen on the log–log scale in the inset of Fig. 3. The power law is in clear contrast to an exponential decay $p(x) \sim \exp(-x/l)$ expected for a normal diffusion of holes, even accounting for any photon-assisted enhancement of the diffusion length l .

3. Discussion

The observed hole distribution $p(x)$ for all temperatures follows the calculated distribution for the Lévy flight random walk governed by the single-step probability (1) evaluated as the photon reabsorption probability [13,15]; it is fully determined by the absorption and the emission spectra. At large distances ($x \gg \alpha_0^{-1}, l$) a tangible contribution to $\mathcal{P}(x)$ results only from the exponentially varying Urbach part of the absorption spectra. This region also correspond to the exponentially decaying red wing of the intrinsic emission spectrum. Assuming the intrinsic spectrum in the VRS form, we find [14,15] an analytic expression for index γ of the single-step distribution

$$\gamma_{\text{VRS}} = 1 - \frac{\Delta}{kT}. \quad (5)$$

Detailed calculations of the emission intensity (which is proportional to the hole concentration) have been extensively discussed in [6,25,26,15]. An analytic expression for the hole distribution $p(x)$ can be derived [27] in the so-called “longest flight” approximation [6,28,27] and is of the form

$$p(x) = \frac{cx_f^\gamma}{x^{1+\gamma}[1 + (x_f/x)^\gamma]^2}, \quad (6)$$

where c is a normalization constant. Distribution (6) provides a good approximation to the exact solution in the entire range of x . Asymptotically (at $x \gg x_f$) it reproduces the single-step probability (1), exhibiting a power-law decay with index γ . At short distances,

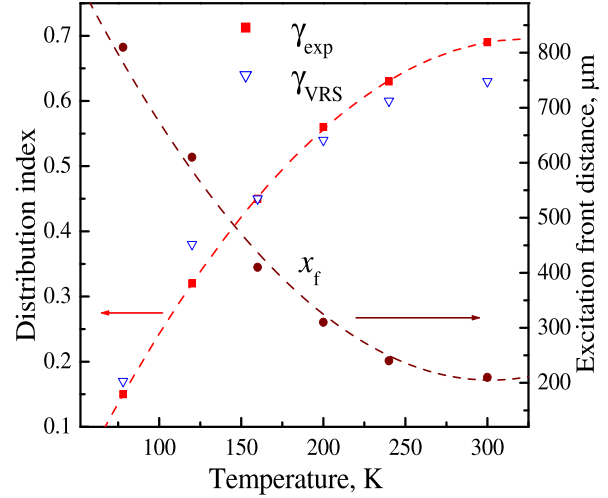


Fig. 4. (Color online.) Temperature dependence of the parameters of Lévy distribution. Index γ shown by squares is estimated from the long-distance asymptotics of the measured $p(x)$; also shown (triangles) are the theoretical values (5). The excitation front distance x_f is estimated from maximum curvature in the log–log plots of Fig. 3. Lines are guides to the eye.

$x \ll x_f$, it gives a weaker decay, $p(x) \propto x^{\gamma-1}$, in agreement with the exact solution [13,27]. The distance x_f gives an estimate of the spread of the excitation “front” of $p(x)$ – beyond which the holes appear predominantly in one step. The transition between the short- and long-distance asymptotics is clearly seen for all T in the inset to Fig. 3, with x_f being the point of maximum curvature in the log–log plots.

We have estimated γ through the slope of log–log variation at far distances and also x_f via the position of maximum curvature of $p(x)$. The temperature variation of obtained values of γ and x_f is shown in Fig. 4. Also shown are theoretical values of the index γ_{VRS} calculated (5) by assuming the intrinsic emission spectrum in the VRS form (3). We see that the estimation of γ through the Urbach tailing parameter gives a good agreement with experiment.

Position of the excitation front can also be estimated [13,15,14] through the recycling factor, viz. $x_f = x_0 \Phi^{1/\gamma}$, where $x_0 \approx 0.2$ μm , is the length scaling parameter of $\mathcal{P}(x)$. The observed huge increase of the excitation front distances, $x_f \gg x_0$ up to the mm-range at low temperatures is another hallmark of Lévy flight, which cannot be attributed to any other mechanism of hole transport. We note however, that for $\Phi \approx 100$ and observed $\gamma(T)$ one should expect even higher increase of x_f . Therefore, our experiments suggest a decreasing recycling factor at lower T . Apparently, the well-known increase of the radiative recombination rate at low T is accompanied by an even faster growth rate of non-radiative recombination, as found for several recombination models with vanishing activation barrier [29–31].

From a practical perspective, the anomalous transport of minority carriers should be important in all semiconductor devices with high radiative efficiency, in particular in light-emission and photo-voltaic devices [15]. However, details of the transport and the temperature effects depend on the absorption spectrum in the tailing region and are not universal, e.g. often deviate from the Urbach shape. Thus, some semiconductors feature Gaussian tails [32]. We have calculated the index γ for Gaussian tails and found it to increase with decreasing temperature, remaining within a narrow range ($0.85 < \gamma < 1.05$) close to unity for a wide temperature variation. Such semiconductors may serve as an experimental model for studying the transition from Lévy flight ($\gamma < 1$) to Lévy walk ($1 < \gamma < 2$). To our knowledge, this transition has been considered only as a notional possibility [18].

From a broader perspective, the photon-mediated transport of holes in high-radiative-efficiency n -InP, owing to its well-controlled and variable SSD index, represents a powerful experimental model for studying subtle effects associated with the Lévy flight. In all previously studied Lévy flight systems, the SSD index was not controllable and certainly not continuously variable. Coupled with the usually limited dynamic range, this made it difficult to distinguish between the inevitable effects of SSD truncation (e.g. due to a finite size of the system), effects of the boundaries and still more complex effects of multi-dimensionality. These subtle effects are now open to systematic investigation.

4. Conclusions

We studied the stationary hole distribution $p(x)$ produced by photo-excitation at an edge of n -InP slab and observed by broad-sided luminescence at temperatures ranging from 300 K to 78 K. We discovered a giant increase of the hole spread in the sample over distances x exceeding 1 cm from the photo-excited edge. A power-law decline of the luminescence intensity characteristic of Lévy flight kinetics is observed with no change in the spectral shape. Our experiment provides a realization of the Lévy flight of holes, in which the Lévy distribution index γ is controlled by the temperature and can be continuously lowered from $\gamma \approx 0.7$ to $\gamma \leq 0.3$ in a regular and well-understood manner. Such a control has never been available for formerly studied Lévy processes.

Acknowledgements

This work was supported by the Domestic Nuclear Detection Office, by the Defense Threat Reduction Agency (basic research program), and by the Center for Advanced Sensor Technology at Stony Brook.

References

- [1] T.H. Solomon, E.R. Weeks, H.L. Swinney, *Phys. Rev. Lett.* 71 (1993) 3975.
- [2] N.E. Humphries, N. Queiroz, J.R.M. Dyer, et al., *Nature* 465 (2010) 1066.
- [3] P. Carr, L. Wu, *J. Financ. Econ.* 71 (2004) 113.
- [4] M.M. Meerschaert, Y. Zhang, B. Baeumer, *Geophys. Res. Lett.* 35 (2008) L17403.
- [5] N. Mercadier, W. Guerin, M. Chevrollier, R. Kaiser, *Nat. Phys.* 5 (2009) 602.
- [6] V.V. Ivanov, Transfer of radiation in spectral lines, Pub. 385, Nat. Bureau Standards, 1973;
- [7] G. Rybicki, A. Lightman, *Radiation Processes in Astrophysics*, Wiley, 1979.
- [8] P. Barthelemy, J. Bertolotti, D.S. Wiersma, *Nature* 453 (2008) 495. Here the power-law index for photon SSD was controlled in an artificial medium with scatterers, separated by spacers of pre-calculated size distribution.
- [9] V.A.A. Jansen, A. Mashanova, S. Petrovskii, *Science* 335 (2012) 918.
- [10] A.M. Edwards, *Ecology* 92 (2011) 1247.
- [11] S. Lepri, A. Politi, *Phys. Rev. E* (2011) 030107(R).
- [12] A.V. Chechkin, V.Yu. Gonchar, R. Gorenflo, N. Korabel, I.M. Sokolov, *Phys. Rev. E* (2008) 021111.
- [13] B.N.N. Achar, J.W. Hanneken, *J. Mol. Liq.* 114 (2004) 147.
- [14] S. Luryi, O. Semyonov, A.V. Subashiev, Z. Chen, *Phys. Rev. B* 86 (2012) 201201(R).
- [15] O. Semyonov, A.V. Subashiev, Z. Chen, S. Luryi, *J. Lumin.* 132 (2012) 1935.
- [16] S. Luryi, A.V. Subashiev, *Int. J. High Speed Electron. Syst.* 21 (2012) 1250001, arXiv:1202.5576.
- [17] J.-P. Bouchaud, A. Georges, *Phys. Rep.* 195 (1990) 127.
- [18] M. Shlesinger, G. Zaslavsky, U. Frisch (Eds.), *Lévy Flights and Related Topics in Physics*, Springer, 1995.
- [19] R. Metzler, J. Klafter, *Phys. Rep.* 339 (2000) 1.
- [20] A. Subashiev, O. Semyonov, Z. Chen, S. Luryi, *Appl. Phys. Lett.* 97 (2010) 181914.
- [21] O. Semyonov, A.V. Subashiev, Z. Chen, S. Luryi, *J. Appl. Phys.* 108 (2010) 013101.
- [22] ACROTEC InP wafers from NIKKO Metals, Japan.
- [23] W. van Roosbroek, W. Shockley, *Phys. Rev.* 94 (1954) 1558.
- [24] Unfortunately, this detailed comparison cannot be extended to lower temperatures, since the absorption spectra are not known in the whole energy range of interest. See, however, [24].
- [25] O. Semyonov, A.V. Subashiev, Z. Chen, S. Luryi, *J. Lumin.* (2013), <http://dx.doi.org/10.1016/j.jlumin.2013.11.002>, also arXiv:1306.2928.
- [26] L.M. Biberman, *Zh. Eksp. Teor. Fiz.* 17 (1947) 416, *Sov. Phys. JETP* 19 (1949) 584.
- [27] T. Holstein, *Phys. Rev.* 72 (1947) 1212.
- [28] A. Subashiev, S. Luryi, in: *Future Trends in Microelectronics: Frontiers and Innovations*, Wiley, 2013, p. 359, arXiv:1212.3001.
- [29] S. Foss, D. Korshunov, S. Zachary, *An Introduction to Heavy-Tailed and Subexponential Distributions*, Springer, 2011. In the mathematical literature this approximation is known as the "single big jump principle".
- [30] V. Abakumov, V.I. Perel, I.N. Yassievich, *Non-radiative Recombination in Semiconductors*, Elsevier Science, 1991.
- [31] I. Tsimberova, Y. Rosenwaks, M. Molotskii, *J. Appl. Phys.* 93 (2003) 9797.
- [32] B. Laikhtman, *J. Appl. Phys.* 112 (2012) 093111.
- [33] P.G. Eliseev, *J. Appl. Phys.* 93 (2003) 5404.